

Graphic Design with Large Multimodal Model

Yutao Cheng^{*1}, Zhao Zhang^{*1}, Maoke Yang^{*1},
Hui Nie^{1,2}, Chunyuan Li¹, Xinglong Wu¹, and Jie Shao^{✉1}

¹ByteDance ²UCAS

{yutao.135,yangmaoke,shaojie.mail}@bytedance.com
zzhang@mail.nankai.edu.cn

Abstract. In the field of graphic design, automating the integration of design elements into a cohesive multi-layered artwork not only boosts productivity but also paves the way for the democratization of graphic design. One existing practice is Graphic Layout Generation (GLG), which aims to layout sequential design elements. It has been constrained by the necessity for a predefined correct sequence of layers, thus limiting creative potential and increasing user workload. In this paper, we present Hierarchical Layout Generation (HLG) as a more flexible and pragmatic setup, which creates graphic composition from *unordered* sets of design elements. To tackle the HLG task, we introduce Graphist, the first layout generation model based on large multimodal models. Graphist efficiently reframes the HLG as a sequence generation problem, utilizing RGB-A images as input, outputs a JSON draft protocol, indicating the coordinates, size, and order of each element. We develop multiple evaluation metrics for HLG. Graphist outperforms prior arts and establishes a strong baseline for this field. Project homepage: <https://github.com/graphic-design-ai/graphist>

Keywords: Graphic design · Layout generation · LMM · MLLM

1 Introduction

Graphic design [41] fundamentally serves as a form of visual communication. It involves the creation and combination of symbols, images, and text to express certain ideas or messages. This field requires significant expertise and time investment to produce aesthetically pleasing graphic compositions. Recently, there is a significant paradigm shift in leveraging AI for automating the layout of given design elements into cohesive graphic compositions heralds [26, 27, 90, 100]. This could potentially reduce the workload of professional designers and provide an avenue for beginners to create their design pieces, making graphic design more democratize and effective.

A preliminary attempt to automate this process is observed in the task known as **Graphic Layout Generation (GLG)** [16, 25, 30, 35, 39, 40, 52–54, 83, 86, 97]. GLG

* Equal Contributions



Fig. 1: Schematic diagram of hierarchical layout generation. (Left) A comparison between the traditional *GLG* task and the newly proposed *HLG* task, with the major difference in that *HLG* relaxes the constraint of *GLG*, so that unordered multimodal input elements can be processed. (Right) Errors in either layer sequencing or spatial positioning can significantly impact the overall quality of the design.

attempts to intelligently arrange provided elements into attractive compositions under the assumption of a *predefined order of layers*. However, establishing the appropriate ordering of these layers is a design cornerstone that, if mismanaged, can fracture the visual hierarchy, leading to disarray in the intended message delivery. Requiring users to prescribe an accurate layer sequence prior to layout not only burdens them with foresight and planning but also stifles layout algorithms, restricting their capacity to transcend such confines in the pursuit of innovative and aesthetically superior outcomes.

In pursuit of more practical applications, this paper introduces a new task, **Hierarchical Layout Generation (HLG)**. *HLG* to craft a visually appealing graphic composition from a collection of unordered elements by meticulously considering both their spatial arrangement and the sequencing of layers. The adjective *hierarchical* emphasizes the significance of element ordering, setting *HLG* apart from conventional layout generation practices. The distinction between *GLG* and *HLG* is illustrated in the left panel of Figure 1, while the right panel of the same figure captures the impact of layer sequencing and spatial positioning on the visual aesthetics of graphic design.

For the *HLG* task, we introduce Graphist, the first layout generation model built upon Large Multimodal Model (LMM) [13, 18, 49, 57, 70, 104]. The layout generation task is challenging that it digests diverse input elements such as RGB-A materials, RGB images, and texts, and the desired outcomes must precisely reflect the intricate relationships among these multimodal input elements. LMMs are well-suited for this task, as they can unify different modalities, like images, text, coordinates [13, 64] into tokens. This allows for flexible configuration of various tasks, such as *HLG*, *GLG*, and more variants. The knowledge and strong reasoning ability stored in pre-trained model parameters are also beneficial for layout tasks. Furthermore, LMMs demonstrate significant potential for scaling [42, 61, 73], enabling the pursuit of enhanced performance through the use of larger models and more extensive datasets. For these reasons, LMMs were

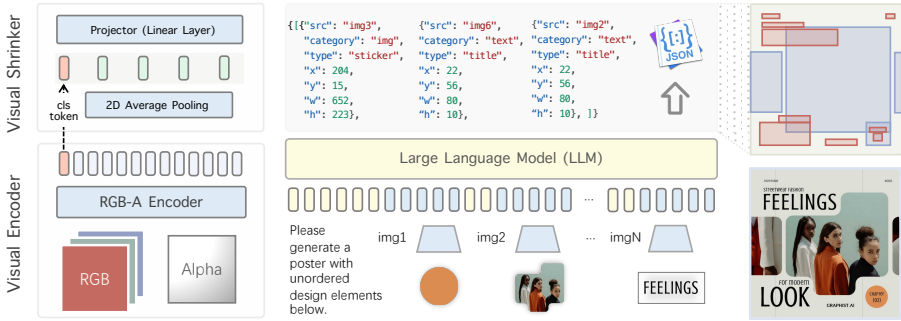


Fig. 2: Graphist Pipeline. Graphist comprises three components: RGB-A Encoder, Visual Shrinker, and a LLM. It accepts a variety of design elements and generates a graphic composition in JSON format end-to-end.

a natural choice for our foundational architecture in developing Graphist. In our specific approach for HLG, we train Graphist with graphic composition data, in which, as shown in Figure 2, each design element is represented as an RGB-A image as input, the model then generates a JSON draft protocol, which specifies the coordinates, size, order and other attributes of each design elements in end-to-end manner.

To evaluate the HLG task, we introduce two novel metrics: Inverse Order Pair Ratio (IOPR) and GPT-4V Eval. The former assesses the accuracy of the layer order in the graphic composition, while the GPT-4V Eval, leveraging the capabilities of GPT-4V [62], quantifies the overall aesthetic quality. Additionally, we have incorporated a human rating score to align with the subjective perceptions of real individuals. Graphist has emerged as the SoTA solution, excelling across all these metrics. Furthermore, Graphist consistently delivers impressive performance on conventional GLG task.

We summarize our contributions as follows:

- We introduce the Hierarchical Layout Generation (HLG) task, which creates graphic compositions from unordered design elements. HLG overcomes the constraints of the Graphic Layout Generation that requires pre-determined layer ordering. The new setup allows more flexible and practical AI-assisted graphic designs.
- We present Graphist, the first LMM-parameterized layout generation model that can be trained end-to-end. Graphist accepts a variety of vision-and-language multimodal design elements and generates a graphic compositions in JSON code format, which can be further automatically rendered into the final design.
- We develop evaluation metrics for HLG, including IOPR and GPT-4V Eval. Graphist shows superior performance in these metrics, setting a robust benchmark for the field.

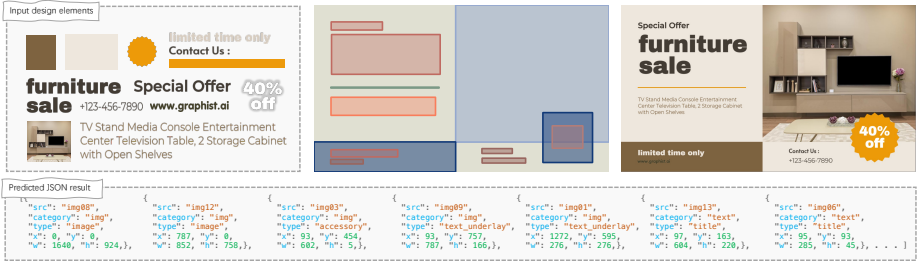


Fig. 3: A user-generated case via graphist web demo. The top-left figure represents the input design elements to Graphist. Below it, we present the corresponding output JSON code generated by Graphist. The final two images in the top row illustrate the visualized results: first is the layout visualization, and the second is the graphic composition by putting these elements according to the JSON protocol. Additional examples are available in Figure 6.

2 Related Work

2.1 Graphic Layout Generation

Graphic design is a form of visual art that combines multimodal elements (*e.g.*, images, texts, and symbols) to create aesthetically pleasing compositions which can effectively convey information to the audience. As one of the core technologies in automated graphic design, layout generation methods has been widely used in various scenarios, such as document [39, 100], UI [6, 19, 58, 82], social media snippets [90], banners [44], poster and advertisement [30, 52, 55], icon/logo [11, 24, 59, 85], CAD Sketches [27, 63], slides [26, 32, 68].

As people deepen their understanding of layout generation tasks, the modeling of layout generation problems is becoming increasingly complex. Early methods for layout generation typically relied on aesthetic rules [5, 87] or constraints [34, 37]. However, the diversity and aesthetics of generated compositions are primarily restricted by the formalized human prior knowledge, and are hard to scale up for production. Later on, some data-driven methods [2, 44, 47] emerged, utilizing learning-based generation models for layout generation. These approaches are dedicated to fitting the data distribution of the topological relationship between elements, and focus on the alignment of elements, but neglecting the content of the elements. Recent methods [12, 29, 46, 55, 92, 101] have recognized the importance of element content, and have explored ways to layout text or decorations on a given base graphic without obstructing important content. Drawing from this observation, attempts [36, 99] have also been made to incorporate multimodal inputs in order to better understand the content of each layer. These methods often assume that the layering order of the elements has been predefined [36, 86], which is difficult to achieve in the practical application. Therefore, we argue that the layer ordering needs to be fully considered in the layout generation problem.

The advancement of layout generation techniques is closely intertwined with the progress of fundamental algorithms. During the early exploration [5, 34, 37, 87], researchers attempted to define beauty using formulas and constraints. Subsequently, generative methods based on GANs [31, 47, 48], VAEs [2, 44], and diffusions [46, 82, 97] have been widely attempted. Besides, LayoutDETR [92] combining DETR [10] and generative models has been attempted to deal with the problem of element arrangement on a given image. In the era of Transformer [77], several methods [36, 39, 53] have adopted the powerful learning capabilities of Transformers to address layout and related control problems [39, 53]. FlexDM [36] models graphic design using a BERT-like [20] approach. The rise of large language models [9, 75, 76] has also captured the attention of researchers in the field of graphic design, with LayoutPrompter [54] and LayoutNUWA [72] introducing language models into layout generation in a zero-shot manner. COLE [38] fuses large language models and diffusion models to build a hierarchical graphic design framework. Our approach is also inspired by large language models [76, 98] and multimodal models [13, 56, 57, 104]. However, COLE [38] focuses on utilizing the generating power of diffusion models to directly produce multi-layer graphic designs based on user intent, while our approach prioritizes the use of existing design elements for layout generation.

2.2 Large Multimodal Models

As a bridge between language and vision, LMM [45, 89, 95] has received widespread attention recently. Related topic including autonomous driving [17, 21], video understanding [50, 71, 96], open-vocabulary vision understanding [51, 84, 93], multimodal agent [78, 88], image generation [7, 69, 94], embodied intelligence [8, 23, 60] and so on. To the best of our knowledge, Graphist is the first work to address the task of layout generation using LMM in an end-to-end manner. While COLE [38] likewise employs multimodal models in their pipeline, their main emphasis lies in generating text content and styles on predetermined base image.

Common architectures of LMM typically encompass a pre-trained visual encoder [22, 67] for extracting visual features, a pre-trained LLM [74–76] for interpreting user commands and generating responses, as well as a vision-language cross-modal connector [1, 28, 49, 57, 103] for aligning the visual encoder outputs to the language model. Given that the task of hierarchical layout generation involves organizing design elements on a blank canvas, the compatibility of coordinates is of paramount importance. Pix2Seq [15] was the first to explore the use of a discretization and serialization approach in object detection problems, in order to convert coordinates into token sequences that can ultimately be used in sequence generation mode. Some work, like OFA [79], VisionLLM [81], Kosmos-2 [33], build upon this form by introducing special coordinate tokens in their vocabulary. Alternatively, PerceptionGPT [65] implements an additional vision encoder and decoder specifically for processing and predicting coordinates. Most notable among these approaches is Shikra [13], which represents spatial positions using numerical values in natural language. It has been proven succinct and effective, as echoed by related research [4, 80, 91]. Inspired by Shikra, our

work adopts the numerical representation for coordinates in the natural language sequence.

3 Task Formulation

3.1 Graphic Layout Generation

For a unified representation, we assume that a text box can be represented by an RGB-A image, which can usually be achieved through rendering or similar methods. Under this assumption, GLG is defined as finding an optimal arrangement for a collection of RGBA design assets $\mathcal{M} = \{M_i \in \mathbb{R}^{h_i \times w_i \times 4}\}_{i=1}^n$. This endeavor seeks to spatially organize the set in a coherent graphic composition $\mathcal{S} = \{s_i\}_{i=1}^n = f(\mathcal{M})$, where $f(\cdot)$ embodies our Graphist layout methodology. Specifically, the output constitutes a set of transformations wherein for each asset M_i , a quadruple (x_i, y_i, w_i, h_i) expresses its upper-left corner placement along with the respective width and height adjustments within the composition.

3.2 Hierarchical Layout Generation

Given a set of RGB-A design elements $\mathcal{M} = \{M_i \in \mathbb{R}^{h_i \times w_i \times 4}\}_{i=1}^n$, HLG seeks to arrange them into a well-constructed graphic composition $\mathcal{S} = \{s_i\}_{i=1}^n = f(\mathcal{M})$. In this context, $f(\cdot)$ denotes the layout action implemented by our method, which we refer to as Graphist. Each element s_i in the layout prediction encompasses five numerical values $(x_i, y_i, w_i, h_i, l_i)$, associated with M_i top/left coordinates, width, height and hierarchy respectively. As shown in Figure 1, compare to conventional GLG task [86], HLG framework emphasizes the significance of element stratification by imposing a hierarchy l_i that dictates not only the placement but also the z -order of each element, thus ensuring a compositionally harmonious layering.

4 Proposed Method

4.1 Graphist Architecture

Graphist is constructed using a LMM, which receives the input of multimodal design elements and predicts a JSON fragment formatted like Figure 2. Graphist comprises three components: (i) *RGBA-Encoder*. We utilize a ViT-L/14 with 224×224 four-channel input as RGBA-Encoder, initialized with visual tower parameters of CLIP [67], excluding the alpha channel. (ii) *LLM*. Our LLM foundation incorporates Qwen1.5-0.5B/7B [3]. (iii) *Visual Shrinker*. To manage the extensive elements processing requirements of Graphist, the Visual Shrinker compresses ViT’s $16 \times 16 + 1$ (cls-token) output grid feature tokens into only 5 tokens, thereby saving computational costs. Specifically, it compress the 2D output of ViT’s 16×16 into 2×2 tokens via 2D average pooling and concatenates it with the cls-token to form $\mathbf{V} \in \mathbb{R}^{5 \times D}$. Consequently, it uses one

Table 1: Implementation details including training stages, datasets, and essential parameters: “BS” for batch size, “Length” for total sequence length. “Graphist” is trained on academic data; “Graphist*” on proprietary data. “PE.” denotes the Patch Embedding Layer. “Cap.” signifies image captioning task. “Vari.” denotes the task variants in Section 5.1. “IH-RGBA” is in-house image-text dataset, where images with alpha channel. “IH-Design” is 80k in-house Graphic Design Dataset like Crello [86].

Stage	BS	Length	Tune Part	Task	Training datasets	
					Graphist	Graphist*
1	128	1536	PE Projector	Cap. HLG	ShareGPT4v [14] Flickr30k [66] Crello [86]	+ IH-RGBA
2	64	2048	Projector LLM	Cap. HLG	ShareGPT4v [14] Flickr30k [66] Crello [86]	+ IH-RGBA + IH-Design
3	64	3584	Projector LLM	Cap. HLG GLG Vari.	ShareGPT4v [14] Flickr30k [66] Crello [86] CGL-V2 [46]	+ IH-RGBA + IH-Design

MLP layer to map the \mathbf{V} to $\mathbf{V}' \in \mathbb{R}^{5 \times D'}$ for modal alignment and dimension matching of LLM, where D' is the word embedding dimension defined by LLM. Visual embedding can be inserted into anywhere of input sequence. Inspired by Shikra [13], we employ the digital tokens to represent coordinates, devoid of any vocab, specialty encoders, or any pre-/post-detectors for encoding position information. Model variants include Graphist-Tiny utilizing Qwen1.5-0.5B and Graphist-Base engaging Qwen1.5-7B.

4.2 Training Strategy

The proposed Graphist is trained in three stages. Initially, Stage-1 targets the patch embedding layer and the projector layer. The focal training tasks during this phase predominantly encompass image captioning and the HLG task, leveraging a substantial batch size coupled with a reduced sequence length for efficiency. The primary objectives is to calibrate the visual encoder to interpret the alpha channel in RGB-A imagery and to align the projector with both visual and linguistic features.

Progressing to Stage-2, the training expands to encompass both the projector layer and the full LLM. Training tasks from the initial stage are retained; however, the HLG task is administered with greater frequency to highlight the model’s fundamental understanding of graphic layout.

Finally, in Stage-3, maintains the focus on the projector layer and the complete LLM, but aiming to adapt the model to a broader range of graphic design task types. Traditional GLG task is also regarded as a specific task type in this stage. We list primary configurations during training in Table 1.

To train the model to arrange inputs layer order and spatial coordinates, we randomly shuffle the input elements with a 0.75 probability for all of the Graphic Design datasets used in the training process. In these three stages, the first stage trains 10k steps, while the second and third stages both train 20k steps. The training for the Graphist-Base is over the course of 5 days, whereas for the Graphist-Tiny model, a shorter duration of 2 days is anticipated.

5 Experiment

5.1 Datasets

Crello. [86] Crello dataset ¹ furnishes an array of graphic compositions derived from a web-based design utility, namely Crello (Now change the name to VistaCreate²). It covers an extensive range of graphic compositions suited for various applications such as social media infographics, digital banner ads, blog headers, and printed poster templates. Inside the dataset, each graphic composition includes detailed information about the layering order, spatial positioning, and categorical details of the design elements. The dataset is advantageous for tasks like GLG and has been the foundation for several methods [36, 86]. Additionally, it is a good playground for HLG task. In Flex-DM [36], the dataset is partitioned into 19,095 training, 1,951 validation, and 2,375 testing examples. However, they used the Crello v2, but since the current version released by Crello is v4, we used the intersection of all parts in the two version test sets, a total of 242 graphic compositions as the test set in experiments.

CGL-Dataset V2 is an extension of the CGL-Dataset [102] and provides a dataset for generating advertising poster layouts, including 60,548 training samples and 1,035 testing samples. Previous work [46] has built two tasks based on this dataset: the Content-Aware task and the Content-Agnostic task. In the Content-Aware task, the model is challenged with an input image and textual content, and is required to output the positions of all textual content in the image while autonomously adding underlay and decorative information. The Content-Agnostic task, on the other hand, only requires an image as input. In this case, the model autonomously determines the output, which includes text, underlay, decoration, and other relevant layering information. Graphist has integrated these tasks alongside HLG/GLG tasks to facilitate comparison across a broader spectrum of layout methods [35, 43, 46, 47, 101].

5.2 Evaluation Metrics

Inverse order pair ratio (IOPR). The appropriate order of layers is crucial for the results of HLG. We develop IOPR, which is a ratio representing the

¹ <https://huggingface.co/datasets/cyberagent/crello>

² <https://create.vista.com/>

fraction of overlap element pairs that are in inverse order according to the model’s predictions out of all possible overlapping element pairs. It is calculated as

$$\text{IOPR} = \frac{\sum_{i=1}^{n-1} \sum_{j=i+1}^n \mathbb{1}(\mathcal{O}_j < \mathcal{O}_i \wedge \mathbb{1}(i, j))}{\sum_{i=0}^{n-1} \sum_{j=i+1}^n \mathbb{1}}, \quad (1)$$

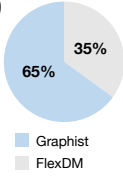
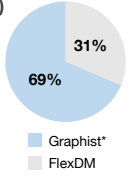
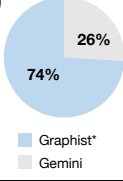
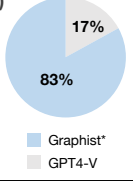
where n is the number of layers in the hierarchical structure. $\mathbb{1}$ is an indicator function that returns 1 if the argument condition is true and 0 otherwise. \mathcal{O} denotes the output order or predicted order of the layers as determined by the model. \mathcal{O}_i and \mathcal{O}_j correspond to the predicted order positions of the i^{th} and j^{th} layers, respectively. $\text{overlap}(i, j)$ is a predicate function that determines whether the i^{th} and j^{th} layers overlap. A low IOPR would suggest that the model is quite accurate in predicting the correct order of layers because there are few inverse order pairs. Contrastingly, a high IOPR would suggest the model often predicts the wrong sequence, indicating lower prediction accuracy. In our experiments, we employed IOPR_{\min} and IOPR_{avg} to evaluate the performance of the model, representing respectively the average score and the minimum score in the test dataset. While the average IOPR across a dataset can provide significant insights, it should be noted that variances in layer orders for specific graphic compositions, when compared to ground truth, do not inherently imply subpar layout performance.

GPT-4V Eval. In addition to the layers order, the overall aesthetic quality and harmony of the elements in the graphic composition are vitally important. We utilize GPT-4V to evaluate our approach and compare it with other alternatives. Following COLE [38], we use four scores named GPT-4V rating including S_{DL} , S_{GI} , S_{IO} and S_{TV} use GPT-4V to evaluate the quality of the graphic composition we generate.

- S_{DL} means the graphic design should present a clean, balanced, and consistent layout. The organization of elements should enhance the message, with clear paths for the eye to follow.
- S_{GI} reflects that any graphics or images used should enhance the design rather than distract from it. They should be high quality, relevant, and harmonious with other elements.
- S_{IO} evaluates the innovation level of the design.
- S_{TV} represents text readability. A lower score would be assigned if the readability of the text is poor due to the color of the text being similar to the background color or overlapping of the text.

As a supplement to GPT-4V rating [38], we propose GPT-4V voting. Here, GPT-4V also partakes in a comparative analysis. It selects the most proficient graphic composition when confronted with two competing outputs. This preference distribution acts as a testament to the discernibility of GPT-4V in recognizing and preferring one method over the other across a range of comparative samples. GPT-4V rating [38] and GPT-4V voting together form the GPT-4V Eval for evaluating layout ability.

Table 2: GPT-4V Eval on Crello. The table demonstrates the performance of different methods on the Crello dataset. Graphist is Graphist-Base built upon Qwen1.5-7B. The scores on the left are GPT-4V rating and IOPR_{avg}, while the chart on the right showcases a comparative evaluation using GPT-4V voting against the FlexDM [36], Gemini-1.5-Pro (Gemini) and GPT-4V. Flex-DM is compared based on the GLG task (a, b), while Gemini-1.5-Pro and GPT-4V are based on the HLG task (c, d).

Method	Task	S_{DL}	S_{GI}	S_{IO}	S_{TV}	IOPR	
Flex-DM	GLG	5.43	6.13	4.69	4.60	-	(a) 
GPT-4V	GLG	5.10	5.83	4.54	3.84	-	
Gemini	GLG	4.87	5.62	4.39	4.09	-	(b) 
Graphist	GLG	5.60	6.64	4.84	4.86	-	
Graphist*	GLG	5.72	6.70	5.03	5.37	-	(c) 
GPT-4V	GLG	4.19	4.66	3.71	3.25	0.45	
Gemini	GLG	5.06	5.94	4.33	4.21	0.70	(d) 
Graphist	HLG	5.66	6.60	5.02	4.93	0.96	
Graphist*	HLG	5.85	6.90	5.10	5.24	0.97	

5.3 Comparison with SoTA

We trained our model using the approach outlined in Section 4.2 and compared it to other state-of-the-art methods. In the following comparison, we represent the model trained only on public datasets as “Graphist”, while “Graphist*” denotes the model trained on in-house data in addition to public datasets.

Results in GLG & HLG tasks. The Crello dataset evaluation underscores the dominance of Graphist* and Graphist over Flex-DM across both tasks. In the GLG task, Graphist* achieved the highest scores in three out of four domains, with marked gains in S_{GI} , attaining a commanding 6.70, and similarly impressive performance in S_{DL} (5.72) and S_{IO} (5.03). In S_{TV} , Graphist* rendered a commendable score, highlighting the method’s robustness in maintaining text readability amidst complex designs. Shifting to the more challenging HLG task, Graphist* not only continued its strong showing but exhibited even more dramatic enhancements, scoring uniformly higher over the counterpart, Flex-DM. Noteworthy is the peak score of 5.85 for S_{DL} , underscoring Graphist*’s proficiency in clean and balanced layout generation. This version also excelled notably in graphic-image synergy with a top score of 6.90 in S_{GI} and innovation with a superior score of 5.10 in S_{IO} . Moreover, the S_{TV} metric remains above Flex-DM, reflecting the model’s diligence in preserving text clarity across design variations. We also evaluate the performance of top-tier proprietary linear mixed models, specifically Gemini-1.5-Pro (Gemini) and GPT-4V, on both tasks. Although they offer greater versatility, there is a significant performance gap compared to our Graphist on layout-centric tasks, such as GLG and HLG.



Fig. 4: Results visualization of the GLG task on the Crello dataset. The results for Flex-DM were derived from their open-source code, whereas the results for GPT-4V and Gemini-1.5-Pro are obtained in zero-shot manner.

Regarding the evaluation details, there may be situations where GPT-4V and Gemini-1.5-Pro cannot correctly infer the required JSON format. We have prepared format post-processing for their common return result types, and we give these two methods five inference opportunities for each test case. If all are unsuccessful, then skip. In the end, GPT-4V retained 120 results, and Gemini-1.5-Pro retained 240 results. We reported their scores on these subsets.

In the visualization of the GLG outcomes in Figure 4, Graphist outperforms competitors including Flex-DM, GPT-4V, and Gemini-1.5-Pro. The other methodologies grapple with challenges such as text overlap and image distortion. Furthermore, we evaluated real-world design elements, contrasting the performance of Gemini-1.5-Pro with Graphist, as depicted in Figure 5. For complex design tasks involving over ten layers, our approach yield more refined design outcomes. Although Gemini-1.5-Pro managed to accomplish the HLG task, the design acuity is markedly distinct from that of Graphist.

Results on CGL-V2. Besides the HLG and GLG tasks, our model can adapt to various other design tasks through flexible configurations. We conducted Content-Aware and Content-Agnostic layout generation experiments on the CGL-

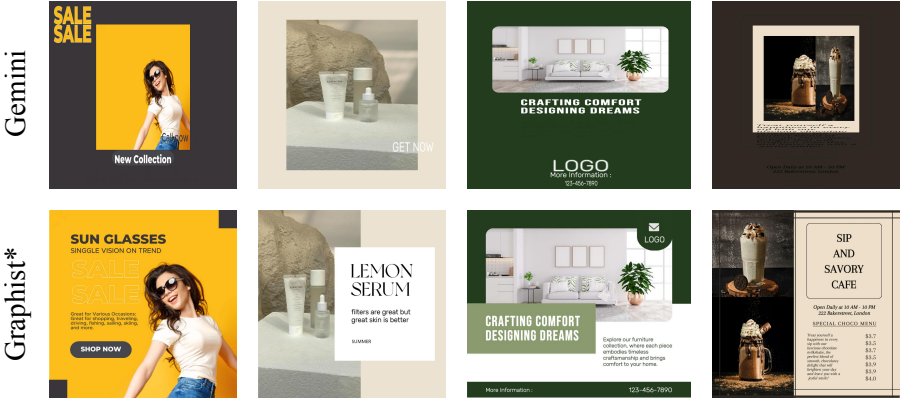


Fig. 5: Comparison with SoTA method on the HLG task with real-world design elements. Both Gemini-1.5-Pro and Graphist models are tasked with HLG using identical real-world design elements. The outcomes indicate superior design quality achieved by our Graphist* when compared with Gemini-1.5-Pro.

Table 3: Comparison with content-aware methods on CGL-V2. In this table, we compare Graphist based on Qwen1.5-7B [3] against other content-aware methods. Content-aware refers to generating a layout based on the input background image and text content. C-R means Composition-relevant.

Method	C-R measures		Graphic measures		
	$R_{com} \downarrow$	$R_{occ} \uparrow$	$R_{ali} \downarrow$	$R_{ove} \downarrow$	$R_{und} \uparrow$
ContentGAN [47]	31.930	1.000	0.009	0.065	0.840
CGL-GAN [101]	16.040	0.875	0.007	0.081	0.732
RADM [46]	10.260	0.997	0.008	0.046	0.983
Graphist*	12.150	1.000	0.004	0.002	0.996

V2 dataset based on Qwen1.5-7B and following the experiment settings and evaluation metrics of [101].

In the Content-Aware layout design, from Table 3, Graphist stands out with the lowest R_{com} of 12.150, the highest R_{occ} tied with ContentGAN at 1.000, and leading performances in all graphic measures ($R_{ali} = 0.004$, $R_{ove} = 0.002$, $R_{und} = 0.996$), indicating superior graphic visual balance, non-emptiness, alignment, overlap avoidance, and underlay success.

Similarly, within Content-Agnostic task, Graphist again showcases its robust capability by achieving the best R_{com} score of 7.074 and perfect R_{occ} score, which is illustrated in Table 4. It also surpasses competitors in graphic measures, underpinning its strength in alignment ($R_{ali} = 0.0003$), minimizing elements overlap ($R_{ove} = 0.001$), and maximizing the informative underlay usage ($R_{und} = 1.0$). These results cement Graphist as a versatile and potent solution

Table 4: Comparison with content-agnostic methods on CGL-V2. In this table, we compare Graphist based on Qwen1.5-7B [3] against other content-agnostic methods. Content-agnostic refers to generating a layout based solely on the background image. C-R means Composition-relevant.

Method	C-R measures		Graphic measures		
	$R_{com} \downarrow$	$R_{occ} \uparrow$	$R_{ali} \downarrow$	$R_{ove} \downarrow$	$R_{und} \uparrow$
BLT [43]	28.540	1.000	0.004	0.002	0.993
LayoutDM [35]	21.300	1.000	0.006	0.039	0.896
RADM [46]	10.260	0.997	0.008	0.046	0.983
Graphist*	7.074	1.000	0.0003	0.001	1.000

Table 5: Different LLM model. Comparison of Qwen1.5-0.5B, Qwen1.5-7B, and InternLM2-7B performance on the Crello dataset.

LLM	S_{DL}	S_{GI}	S_{IO}	S_{TV}	IOPR_{\min}	IOPR_{avg}
Qwen1.5-0.5B	5.44	6.35	4.94	4.60	0.641	0.963
Qwen1.5-7B	5.85	6.90	5.10	5.37	0.667	0.971
InternLM2-7B	5.60	6.50	4.90	5.00	0.476	0.966

for automatic layout generation, exhibiting notable advancements in synthesizing information-rich graphic compositions.

5.4 Ablation Studies

In this section, we delve into a series of ablation studies to examine the underlying factors that influence the layout quality of Graphist. The specific aspects under investigation include the sequencing of input design elements, the choice of language model, the number of visual tokens, and the encoding of transparency through RGB-A image channels.

Influence of input layer sequencing. In Table 2, we show the performance comparison of our method with structured versus unstructured input sequences. The findings indicate that our approach achieves better results in the metrics S_{DL} , S_{GI} , and S_{IO} when dealing with an unordered input. The flexibility introduced by allowing randomness in input ordering contributes to the superior performance observed in S_{DL} and S_{IO} metrics versus a structured sequence. Nevertheless, this unordered approach increases the complexity of text layer placement, reflected by a reduced score in S_{TV} .



Fig. 6: More user-generated designs via graphist web demo. To evaluate usability, we invited numerous non-expert volunteers to upload their design components to our Graphist web demo, resulting in the creation of their own design projects. The image displays a selection of these high-quality outcomes alongside their respective layouts. Within the layout map, various colors signify distinct layer attributes as recognized by the model.

Impact of LLM. In this evaluation, we explore the influence of varying LLM configurations on our layout generation results. Similarly, we carry out experiments using the Crello dataset and the CGL-V2 dataset. We evaluate models with differing capacities: Qwen1.5-0.5B, Qwen1.5-7B, and InternLM2-7B. As demonstrated in Table 5 and Table 6, our experiments underline that within the domain of our tasks, the larger models consistently outperform their smaller counterparts. In addition, different models of the same size also reflect performance differences.

Influence of visual token length. In our method, we typically represent an image using a sequence of 5 visual tokens. To evaluate the effects of increased token quantity, potentially enhancing the image representation’s granularity, we conducted experiments using a 17 tokens format. The composition of 17 tokens includes 1 cls token and 16 visual tokens, achieved by using a 4×4 pooling kernel size. The results presented in Table 7 suggests that lengthening the visual token sequence does not necessarily lead to performance improvements. According to the outcomes, the representation of an image with a quintet of tokens sufficiently captures the necessary information for this specific task.

Table 6: Different LLM model. Comparison of Qwen1.5-7B and InternLM2-7B performance on the CGL-V2 dataset.

LLM	Task	C-R measures		Graphic measures		
		$R_{com} \downarrow$	$R_{occ} \uparrow$	$R_{ali} \downarrow$	$R_{ove} \downarrow$	$R_{und} \uparrow$
InternLM2-7B	Aware	12.803	1.000	0.004	0.002	0.988
Qwen1.5-7B	Aware	12.150	1.000	0.004	0.002	0.996
InternLM2-7B	Agnostic	9.510	1.000	0.004	0.001	0.999
Qwen1.5-7B	Agnostic	7.074	1.000	0.0003	0.001	1.000

Table 7: Different visual token length. Comparison of different sequence length performance on the Crello dataset based on Graphist-Tiny. From our observation, five tokens are sufficient for layout generation.

Length	S_{DL}	S_{GI}	S_{IO}	S_{TV}	$IOPR_{\min}$	$IOPR_{\text{avg}}$
5 tokens	5.44	6.35	4.94	4.60	0.641	0.963
17 tokens	5.47	6.28	4.88	4.67	0.667	0.965

RGB vs. RGB-A. To assess the effect of omitting the alpha channel, we have also tested the model with traditional three-channel RGB images. As illustrated in Table 8, inputs with the additional alpha channel (RGB-A) yield higher-quality outputs with more accurate layer ordering when compared to RGB inputs. The alpha channel provides detailed information that aids the model in discerning textural elements and gradients within the image layers. Importantly, when processing text layers, the alpha channel allows the model to isolate text from potentially distracting backgrounds, facilitating improved clarity and precision in text placement.

5.5 Real-World Evaluation

To assess the real-world applicability of our method, we engaged a group of non-expert volunteers to submit their design assets via our Graphist web demo and chose a selection of representative outputs for analysis. As illustrated in Figure 6, our model successfully generates visually appealing and cohesive designs across varying canvas dimensions and design elements.

5.6 Limitations & Negative Impact

In order to create an efficient design assistant that adheres to user intent, Graphist only represents a starting point. The automatic generation of complete sets of high-quality materials that meet design intent requirements, and

Table 8: Different input channel. Comparison of RGB input and RGB-A input performance on the Crello dataset. The results indicate that RGB-A performs better, particularly in S_{IO} and S_{TV} . This experiment based on Graphist-Tiny model.

Method	S_{DL}	S_{GI}	S_{IO}	S_{TV}	$IOPR_{\min}$	$IOPR_{\text{avg}}$
RGB-A	5.44	6.35	4.94	4.60	0.641	0.963
RGB	5.24	6.14	4.62	4.22	0.502	0.951

the generation of designs that more closely align with human aesthetic preferences, are areas that require further exploration. As we explore more intelligent graphic design systems, potential negative consequences primarily involve generating homogeneous design results and the environmental impact associated with the carbon consumption of model training.

6 Conclusion

This paper represents a step forward from traditional graphic layout generation by introducing the hierarchical layout generation task, which enhances graphic design automation by effectively handling disordered design elements, thereby increasing creative potential and efficiency. To address this more challenging task, we proposed Graphist, a novel LMM that tackles HLG tasks as sequence generation challenges. Graphist takes RGB-A images as input and produces JSON draft protocols that define the layout parameters of graphic compositions. To appropriately evaluate HLG tasks, we introduced two metrics: the Inverse Order Pair Ratio and GPT-4V Eval. Our evaluation metrics demonstrate that Graphist achieves state-of-the-art results, providing a strong baseline for generating automated graphic designs that are more creative and diverse.

References

1. Alayrac, J.B., Donahue, J., Luc, P., Miech, A., Barr, I., Hasson, Y., Lenc, K., Mensch, A., Millican, K., Reynolds, M., et al.: Flamingo: a visual language model for few-shot learning. *Advances in Neural Information Processing Systems* **35**, 23716–23736 (2022)
2. Arroyo, D.M., Postels, J., Tombari, F.: Variational transformer networks for layout generation. In: *CVPR*. pp. 13642–13652 (2021)
3. Bai, J., Bai, S., Chu, Y., Cui, Z., Dang, K., Deng, X., Fan, Y., Ge, W., Han, Y., Huang, F., Hui, B., Ji, L., Li, M., Lin, J., Lin, R., Liu, D., Liu, G., Lu, C., Lu, K., Ma, J., Men, R., Ren, X., Ren, X., Tan, C., Tan, S., Tu, J., Wang, P., Wang, S., Wang, W., Wu, S., Xu, B., Xu, J., Yang, A., Yang, H., Yang, J., Yang, S., Yao, Y., Yu, B., Yuan, H., Yuan, Z., Zhang, J., Zhang, X., Zhang, Y., Zhang, Z., Zhou, C., Zhou, J., Zhou, X., Zhu, T.: Qwen technical report. *arXiv preprint arXiv:2309.16609* (2023)

4. Bai, J., Bai, S., Yang, S., Wang, S., Tan, S., Wang, P., Lin, J., Zhou, C., Zhou, J.: Qwen-vl: A frontier large vision-language model with versatile abilities. arXiv preprint arXiv:2308.12966 (2023)
5. Bauerly, M., Liu, Y.: Computational modeling and experimental investigation of effects of compositional elements on interface and design aesthetics. *International journal of human-computer studies* **64**(8), 670–682 (2006)
6. Beltramelli, T.: pix2code: Generating code from a graphical user interface screenshot. In: *Proceedings of the ACM SIGCHI Symposium on Engineering Interactive Computing Systems*. pp. 1–6 (2018)
7. Betker, J., Goh, G., Jing, L., Brooks, T., Wang, J., Li, L., Ouyang, L., Zhuang, J., Lee, J., Guo, Y., et al.: Improving image generation with better captions. *Computer Science*. <https://cdn.openai.com/papers/dall-e-3.pdf> **2**(3), 8 (2023)
8. Brohan, A., Brown, N., Carbajal, J., Chebotar, Y., Chen, X., Choromanski, K., Ding, T., Driess, D., Dubey, A., Finn, C., et al.: Rt-2: Vision-language-action models transfer web knowledge to robotic control. arXiv preprint arXiv:2307.15818 (2023)
9. Brown, T., Mann, B., Ryder, N., Subbiah, M., Kaplan, J.D., Dhariwal, P., Neelakantan, A., Shyam, P., Sastry, G., Askell, A., et al.: Language models are few-shot learners. *Advances in neural information processing systems* **33**, 1877–1901 (2020)
10. Carion, N., Massa, F., Synnaeve, G., Usunier, N., Kirillov, A., Zagoruyko, S.: End-to-end object detection with transformers. In: *Computer Vision—ECCV 2020: 16th European Conference, Glasgow, UK, August 23–28, 2020, Proceedings, Part I* 16. pp. 213–229. Springer (2020)
11. Carlier, A., Danelljan, M., Alahi, A., Timofte, R.: Deepsvg: A hierarchical generative network for vector graphics animation. *Advances in Neural Information Processing Systems* **33**, 16351–16361 (2020)
12. Chai, S., Zhuang, L., Yan, F., Zhou, Z.: Two-stage content-aware layout generation for poster designs. In: *ACM MM*. pp. 8415–8423 (2023)
13. Chen, K., Zhang, Z., Zeng, W., Zhang, R., Zhu, F., Zhao, R.: Shikra: Unleashing multimodal llm’s referential dialogue magic. arXiv preprint arXiv:2306.15195 (2023)
14. Chen, L., Li, J., Dong, X., Zhang, P., He, C., Wang, J., Zhao, F., Lin, D.: Sharegpt4v: Improving large multi-modal models with better captions. arXiv preprint arXiv:2311.12793 (2023)
15. Chen, T., Saxena, S., Li, L., Fleet, D.J., Hinton, G.: Pix2seq: A language modeling framework for object detection. arXiv preprint arXiv:2109.10852 (2021)
16. Cheng, C.Y., Huang, F., Li, G., Li, Y.: Play: Parametrically conditioned layout generation using latent diffusion. arXiv preprint arXiv:2301.11529 (2023)
17. Cui, C., Ma, Y., Cao, X., Ye, W., Zhou, Y., Liang, K., Chen, J., Lu, J., Yang, Z., Liao, K.D., et al.: A survey on multimodal large language models for autonomous driving. In: *WACV*. pp. 958–979 (2024)
18. Dai, W., Li, J., Li, D., Tiong, A.M.H., Zhao, J., Wang, W., Li, B., Fung, P., Hoi, S.: Instructblip: Towards general-purpose vision-language models with instruction tuning. arXiv preprint arXiv:2305.06500 (2023)
19. Deka, B., Huang, Z., Franzen, C., Hibschan, J., Afegan, D., Li, Y., Nichols, J., Kumar, R.: Rico: A mobile app dataset for building data-driven design applications. In: *Proceedings of the 30th annual ACM symposium on user interface software and technology*. pp. 845–854 (2017)

20. Devlin, J., Chang, M.W., Lee, K., Toutanova, K.: Bert: Pre-training of deep bidirectional transformers for language understanding. arXiv preprint arXiv:1810.04805 (2018)
21. Ding, X., Han, J., Xu, H., Liang, X., Zhang, W., Li, X.: Holistic autonomous driving understanding by bird’s-eye-view injected multi-modal large models. arXiv preprint arXiv:2401.00988 (2024)
22. Dosovitskiy, A., Beyer, L., Kolesnikov, A., Weissenborn, D., Zhai, X., Unterthiner, T., Dehghani, M., Minderer, M., Heigold, G., Gelly, S., et al.: An image is worth 16x16 words: Transformers for image recognition at scale. arXiv preprint arXiv:2010.11929 (2020)
23. Driess, D., Xia, F., Sajjadi, M.S., Lynch, C., Chowdhery, A., Ichter, B., Wahid, A., Tompson, J., Vuong, Q., Yu, T., et al.: PaLM-E: An embodied multimodal language model. arXiv preprint arXiv:2303.03378 (2023)
24. Feng, S., Jiang, M., Zhou, T., Zhen, Y., Chen, C.: Auto-icon+: An automated end-to-end code generation tool for icon designs in ui development. *ACM Transactions on Interactive Intelligent Systems* **12**(4), 1–26 (2022)
25. Feng, W., Zhu, W., Fu, T.j., Jampani, V., Akula, A., He, X., Basu, S., Wang, X.E., Wang, W.Y.: LayoutGPT: Compositional visual planning and generation with large language models. arXiv preprint arXiv:2305.15393 (2023)
26. Fu, T.J., Wang, W.Y., McDuff, D., Song, Y.: DOC2PPT: automatic presentation slides generation from scientific documents. In: *AAAI*. pp. 634–642 (2022)
27. Ganin, Y., Bartunov, S., Li, Y., Keller, E., Saliceti, S.: Computer-aided design as language. *Advances in Neural Information Processing Systems* **34**, 5885–5897 (2021)
28. Gao, P., Han, J., Zhang, R., Lin, Z., Geng, S., Zhou, A., Zhang, W., Lu, P., He, C., Yue, X., et al.: Llama-adapter v2: Parameter-efficient visual instruction model. arXiv preprint arXiv:2304.15010 (2023)
29. Gao, Y., Lin, J., Zhou, M., Liu, C., Xie, H., Ge, T., Jiang, Y.: Textpainter: Multimodal text image generation with visual-harmony and text-comprehension for poster design. In: *ACM MM*. pp. 7236–7246 (2023)
30. Hsu, H.Y., He, X., Peng, Y., Kong, H., Zhang, Q.: PosterLayout: A new benchmark and approach for content-aware visual-textual presentation layout. In: *CVPR*. pp. 6018–6026 (2023)
31. Hsu, H., He, X., Peng, Y.: Densitylayout: Density-conditioned layout gan for visual-textual presentation designs. In: *International Conference on Image and Graphics*. pp. 187–199. Springer (2023)
32. Hu, Y., Wan, X.: Ppsgen: Learning-based presentation slides generation for academic papers. *IEEE transactions on knowledge and data engineering* **27**(4), 1085–1097 (2014)
33. Huang, S., Dong, L., Wang, W., Hao, Y., Singhal, S., Ma, S., Lv, T., Cui, L., Mohammed, O.K., Liu, Q., et al.: Language is not all you need: Aligning perception with language models. arXiv preprint arXiv:2302.14045 (2023)
34. Hurst, N., Li, W., Marriott, K.: Review of automatic document formatting. In: *Proceedings of the 9th ACM symposium on Document engineering*. pp. 99–108 (2009)
35. Inoue, N., Kikuchi, K., Simo-Serra, E., Otani, M., Yamaguchi, K.: LayoutDM: Discrete diffusion model for controllable layout generation. In: *CVPR*. pp. 10167–10176 (2023)
36. Inoue, N., Kikuchi, K., Simo-Serra, E., Otani, M., Yamaguchi, K.: Towards flexible multi-modal document models. In: *CVPR*. pp. 14287–14296 (2023)

37. Jahanian, A., Liu, J., Lin, Q., Tretter, D., O'Brien-Strain, E., Lee, S.C., Lyons, N., Allebach, J.: Recommendation system for automatic design of magazine covers. In: Proceedings of the 2013 international conference on Intelligent user interfaces. pp. 95–106 (2013)
38. Jia, P., Li, C., Liu, Z., Shen, Y., Chen, X., Yuan, Y., Zheng, Y., Chen, D., Li, J., Xie, X., et al.: Cole: A hierarchical generation framework for graphic design. arXiv preprint arXiv:2311.16974 (2023)
39. Jiang, Z., Guo, J., Sun, S., Deng, H., Wu, Z., Mijovic, V., Yang, Z.J., Lou, J.G., Zhang, D.: LayoutFormer++: Conditional graphic layout generation via constraint serialization and decoding space restriction. In: CVPR. pp. 18403–18412 (2023)
40. Jiang, Z., Sun, S., Zhu, J., Lou, J.G., Zhang, D.: Coarse-to-fine generative modeling for graphic layouts. In: AAAI. pp. 1096–1103 (2022)
41. Jobling, P., Crowley, D.: Graphic design: reproduction and representation since 1800. Manchester University Press (1996)
42. Kaplan, J., McCandlish, S., Henighan, T., Brown, T.B., Chess, B., Child, R., Gray, S., Radford, A., Wu, J., Amodei, D.: Scaling laws for neural language models. arXiv preprint arXiv:2001.08361 (2020)
43. Kong, X., Jiang, L., Chang, H., Zhang, H., Hao, Y., Gong, H., Essa, I.: Blt: bidirectional layout transformer for controllable layout generation. In: European Conference on Computer Vision. pp. 474–490. Springer (2022)
44. Lee, H.Y., Jiang, L., Essa, I., Le, P.B., Gong, H., Yang, M.H., Yang, W.: Neural design network: Graphic layout generation with constraints. In: Computer Vision–ECCV 2020: 16th European Conference, Glasgow, UK, August 23–28, 2020, Proceedings, Part III 16. pp. 491–506. Springer (2020)
45. Li, C., Gan, Z., Yang, Z., Yang, J., Li, L., Wang, L., Gao, J.: Multimodal foundation models: From specialists to general-purpose assistants. arXiv preprint arXiv:2309.10020 1(2), 2 (2023)
46. Li, F., Liu, A., Feng, W., Zhu, H., Li, Y., Zhang, Z., Lv, J., Zhu, X., Shen, J., Lin, Z.: Relation-aware diffusion model for controllable poster layout generation. In: Proceedings of the 32nd ACM international conference on information & knowledge management. pp. 1249–1258 (2023)
47. Li, J., Yang, J., Hertzmann, A., Zhang, J., Xu, T.: Layoutgan: Generating graphic layouts with wireframe discriminators. arXiv preprint arXiv:1901.06767 (2019)
48. Li, J., Yang, J., Zhang, J., Liu, C., Wang, C., Xu, T.: Attribute-conditioned layout gan for automatic graphic design. IEEE Transactions on Visualization and Computer Graphics 27(10), 4039–4048 (2020)
49. Li, J., Li, D., Savarese, S., Hoi, S.: Blip-2: Bootstrapping language-image pre-training with frozen image encoders and large language models. arXiv preprint arXiv:2301.12597 (2023)
50. Li, K., He, Y., Wang, Y., Li, Y., Wang, W., Luo, P., Wang, Y., Wang, L., Qiao, Y.: Videochat: Chat-centric video understanding. arXiv preprint arXiv:2305.06355 (2023)
51. Li, X., Yuan, H., Li, W., Ding, H., Wu, S., Zhang, W., Li, Y., Chen, K., Loy, C.C.: Omg-seg: Is one model good enough for all segmentation? arXiv (2024)
52. Li, Z., Li, F., Feng, W., Zhu, H., Liu, A., Li, Y., Zhang, Z., Lv, J., Zhu, X., Shen, J., et al.: Planning and Rendering: Towards end-to-end product poster generation. arXiv preprint arXiv:2312.08822 (2023)
53. Lin, J., Guo, J., Sun, S., Xu, W., Liu, T., Lou, J.G., Zhang, D.: A parse-then-place approach for generating graphic layouts from textual descriptions. In: ICCV. pp. 23622–23631 (2023)

54. Lin, J., Guo, J., Sun, S., Yang, Z.J., Lou, J.G., Zhang, D.: Layout-Prompter: Awaken the design ability of large language models. arXiv preprint arXiv:2311.06495 (2023)
55. Lin, J., Zhou, M., Ma, Y., Gao, Y., Fei, C., Chen, Y., Yu, Z., Ge, T.: Autoposter: A highly automatic and content-aware design system for advertising poster generation. In: Proceedings of the 31st ACM International Conference on Multimedia. pp. 1250–1260 (2023)
56. Liu, H., Li, C., Li, Y., Lee, Y.J.: Improved baselines with visual instruction tuning. arXiv preprint arXiv:2310.03744 (2023)
57. Liu, H., Li, C., Wu, Q., Lee, Y.J.: Visual instruction tuning. arXiv preprint arXiv:2304.08485 (2023)
58. Lu, Y., Tong, Z., Zhao, Q., Zhang, C., Li, T.J.J.: UI layout generation with llms guided by ui grammar. arXiv preprint arXiv:2310.15455 (2023)
59. Mateja, D., Armbruster, R., Baumert, J., Bleil, T., Langenbahn, J., Schwedhelm, J.C., Sester, S., Heinzl, A.: Animatesvg: autonomous creation and aesthetics evaluation of scalable vector graphics animations for the case of brand logos. In: AAAI. pp. 15710–15716 (2023)
60. Mu, Y., Zhang, Q., Hu, M., Wang, W., Ding, M., Jin, J., Wang, B., Dai, J., Qiao, Y., Luo, P.: Embodiedgpt: Vision-language pre-training via embodied chain of thought. *NeurIPS* **36** (2024)
61. OpenAI: Gpt-4 technical report (2023)
62. OpenAI: Gpt-4v(ision) system card (2023), <https://openai.com/research/gpt-4v-system-card>
63. Para, W., Bhat, S., Guerrero, P., Kelly, T., Mitra, N., Guibas, L.J., Wonka, P.: Sketchgen: Generating constrained cad sketches. *Advances in Neural Information Processing Systems* **34**, 5077–5088 (2021)
64. Peng, Z., Wang, W., Dong, L., Hao, Y., Huang, S., Ma, S., Wei, F.: Kosmos-2: Grounding multimodal large language models to the world. arXiv preprint arXiv:2306.14824 (2023)
65. Pi, R., Yao, L., Gao, J., Zhang, J., Zhang, T.: PerceptionGPT: Effectively fusing visual perception into llm. arXiv preprint arXiv:2311.06612 (2023)
66. Plummer, B.A., Wang, L., Cervantes, C.M., Caicedo, J.C., Hockenmaier, J., Lazebnik, S.: Flickr30k entities: Collecting region-to-phrase correspondences for richer image-to-sentence models. In: ICCV. pp. 2641–2649 (2015)
67. Radford, A., Kim, J.W., Hallacy, C., Ramesh, A., Goh, G., Agarwal, S., Sastry, G., Askell, A., Mishkin, P., Clark, J., et al.: Learning transferable visual models from natural language supervision. In: ICML. pp. 8748–8763. PMLR (2021)
68. Shibata, T., Kurohashi, S.: Automatic slide generation based on discourse structure analysis. In: ICON. pp. 754–766. Springer (2005)
69. Sun, Q., Yu, Q., Cui, Y., Zhang, F., Zhang, X., Wang, Y., Gao, H., Liu, J., Huang, T., Wang, X.: Generative pretraining in multimodality. arXiv preprint arXiv:2307.05222 (2023)
70. Tai, Y., Fan, W., Zhang, Z., Liu, Z.: Link-context learning for multimodal llms. In: CVPR (2024)
71. Tang, Y., Bi, J., Xu, S., Song, L., Liang, S., Wang, T., Zhang, D., An, J., Lin, J., Zhu, R., et al.: Video understanding with large language models: A survey. arXiv preprint arXiv:2312.17432 (2023)
72. Tang, Z., Wu, C., Li, J., Duan, N.: Layoutnuwa: Revealing the hidden layout expertise of large language models. arXiv preprint arXiv:2309.09506 (2023)

73. Team, G., Anil, R., Borgeaud, S., Wu, Y., Alayrac, J.B., Yu, J., Soricut, R., Schalkwyk, J., Dai, A.M., Hauth, A., et al.: Gemini: a family of highly capable multimodal models. arXiv preprint arXiv:2312.11805 (2023)
74. Team, I.: Internlm: A multilingual language model with progressively enhanced capabilities. <https://github.com/InternLM/InternLM> (2023)
75. Touvron, H., Lavril, T., Izacard, G., Martinet, X., Lachaux, M.A., Lacroix, T., Rozière, B., Goyal, N., Hambro, E., Azhar, F., et al.: Llama: Open and efficient foundation language models. arXiv preprint arXiv:2302.13971 (2023)
76. Touvron, H., Martin, L., Stone, K., Albert, P., Almahairi, A., Babaei, Y., Bashlykov, N., Batra, S., Bhargava, P., Bhosale, S., et al.: Llama 2: Open foundation and fine-tuned chat models. arXiv preprint arXiv:2307.09288 (2023)
77. Vaswani, A., Shazeer, N., Parmar, N., Uszkoreit, J., Jones, L., Gomez, A.N., Kaiser, Ł., Polosukhin, I.: Attention is all you need. *Advances in neural information processing systems* **30** (2017)
78. Wang, J., Xu, H., Ye, J., Yan, M., Shen, W., Zhang, J., Huang, F., Sang, J.: Mobile-agent: Autonomous multi-modal mobile device agent with visual perception. arXiv preprint arXiv:2401.16158 (2024)
79. Wang, P., Yang, A., Men, R., Lin, J., Bai, S., Li, Z., Ma, J., Zhou, C., Zhou, J., Yang, H.: Ofa: Unifying architectures, tasks, and modalities through a simple sequence-to-sequence learning framework. In: ICML. pp. 23318–23340. PMLR (2022)
80. Wang, W., Lv, Q., Yu, W., Hong, W., Qi, J., Wang, Y., Ji, J., Yang, Z., Zhao, L., Song, X., et al.: Cogvlm: Visual expert for pretrained language models. arXiv preprint arXiv:2311.03079 (2023)
81. Wang, W., Chen, Z., Chen, X., Wu, J., Zhu, X., Zeng, G., Luo, P., Lu, T., Zhou, J., Qiao, Y., et al.: Visionllm: Large language model is also an open-ended decoder for vision-centric tasks. arXiv preprint arXiv:2305.11175 (2023)
82. Wei, J., Courbis, A.L., Lambolais, T., Xu, B., Bernard, P.L., Dray, G.: Boosting gui prototyping with diffusion models. arXiv preprint arXiv:2306.06233 (2023)
83. Weng, H., Huang, D., Zhang, T., Lin, C.Y.: Learn and sample together: Collaborative generation for graphic design layout. In: IJCAI. pp. 5851–5859 (2023)
84. Wu, J., Li, X., Xu, S., Yuan, H., Ding, H., Yang, Y., Li, X., Zhang, J., Tong, Y., Jiang, X., et al.: Towards open vocabulary learning: A survey. *IEEE Transactions on Pattern Analysis and Machine Intelligence* (2024)
85. Wu, R., Su, W., Ma, K., Liao, J.: Iconshop: Text-guided vector icon synthesis with autoregressive transformers. *ACM Transactions on Graphics (TOG)* **42**(6), 1–14 (2023)
86. Yamaguchi, K.: Canvasvae: Learning to generate vector graphic documents. In: ICCV. pp. 5481–5489 (2021)
87. Yang, X., Mei, T., Xu, Y.Q., Rui, Y., Li, S.: Automatic generation of visual-textual presentation layout. *ACM Transactions on Multimedia Computing, Communications, and Applications (TOMM)* **12**(2), 1–22 (2016)
88. Yang, Z., Liu, J., Han, Y., Chen, X., Huang, Z., Fu, B., Yu, G.: Appagent: Multimodal agents as smartphone users. arXiv preprint arXiv:2312.13771 (2023)
89. Yin, S., Fu, C., Zhao, S., Li, K., Sun, X., Xu, T., Chen, E.: A survey on multimodal large language models. arXiv preprint arXiv:2306.13549 (2023)
90. Yin, W., Mei, T., Chen, C.W.: Automatic generation of social media snippets for mobile browsing. In: Proceedings of the 21st ACM international conference on Multimedia. pp. 927–936 (2013)

91. You, H., Zhang, H., Gan, Z., Du, X., Zhang, B., Wang, Z., Cao, L., Chang, S.F., Yang, Y.: Ferret: Refer and ground anything anywhere at any granularity. arXiv preprint arXiv:2310.07704 (2023)
92. Yu, N., Chen, C.C., Chen, Z., Meng, R., Wu, G., Josel, P., Niebles, J.C., Xiong, C., Xu, R.: Layoutdetr: Detection transformer is a good multimodal layout designer. arXiv preprint arXiv:2212.09877 (2022)
93. Yuan, Y., Li, W., Liu, J., Tang, D., Luo, X., Qin, C., Zhang, L., Zhu, J.: Osprey: Pixel understanding with visual instruction tuning. arXiv preprint arXiv:2312.10032 (2023)
94. Zhan, J., Dai, J., Ye, J., Zhou, Y., Zhang, D., Liu, Z., Zhang, X., Yuan, R., Zhang, G., Li, L., et al.: Anygpt: Unified multimodal llm with discrete sequence modeling. arXiv preprint arXiv:2402.12226 (2024)
95. Zhang, D., Yu, Y., Li, C., Dong, J., Su, D., Chu, C., Yu, D.: Mm-llms: Recent advances in multimodal large language models. arXiv preprint arXiv:2401.13601 (2024)
96. Zhang, H., Li, X., Bing, L.: Video-llama: An instruction-tuned audio-visual language model for video understanding. arXiv preprint arXiv:2306.02858 (2023)
97. Zhang, J., Guo, J., Sun, S., Lou, J.G., Zhang, D.: LayoutDiffusion: Improving graphic layout generation by discrete diffusion probabilistic models. In: ICCV (2023)
98. Zhang, P., Zeng, G., Wang, T., Lu, W.: TinyLLaMA: An open-source small language model. arXiv preprint arXiv:2401.02385 (2024)
99. Zheng, X., Qiao, X., Cao, Y., Lau, R.W.: Content-aware generative modeling of graphic design layouts. ACM Transactions on Graphics (TOG) **38**(4), 1–15 (2019)
100. Zhong, X., Tang, J., Yepes, A.J.: Publaynet: largest dataset ever for document layout analysis. In: 2019 International Conference on Document Analysis and Recognition (ICDAR). pp. 1015–1022. IEEE (2019)
101. Zhou, M., Xu, C., Ma, Y., Ge, T., Jiang, Y., Xu, W.: Composition-aware graphic layout gan for visual-textual presentation designs. arXiv preprint arXiv:2205.00303 (2022)
102. Zhou, M., Xu, C., Ma, Y., Ge, T., Jiang, Y., Xu, W.: Composition-aware graphic layout GAN for visual-textual presentation designs. In: IJCAI. pp. 4995–5001. ijcai.org (2022)
103. Zhou, Q., Wang, Z., Chu, W., Xu, Y., Li, H., Qi, Y.: InfMLLM: A unified framework for visual-language tasks. arXiv preprint arXiv:2311.06791 (2023)
104. Zhu, D., Chen, J., Shen, X., Li, X., Elhoseiny, M.: Minigpt-4: Enhancing vision-language understanding with advanced large language models. arXiv preprint arXiv:2304.10592 (2023)